

Asthma Airway Morphology and Hyperpolarized ³He Magnetic Resonance Imaging Ventilation Defects

Sarah Svenningsen^{1,2}, Danielle Starr¹, Harvey Coxson³, Nigel Paterson⁴, David G McCormack⁴, Miranda Kirby^{1,2}, and Grace Parraga^{1,2}

¹Imaging Research Laboratories, Robarts Research Institute, London, Ontario, Canada, ²Department of Medical Biophysics, The University of Western Ontario, London, Ontario, Canada, ³James Hogg Research Centre, University of British Columbia, Vancouver, British Columbia, Canada, ⁴Division of Respiratory, Department of Medicine, The University of Western Ontario, London, Ontario, Canada

Target Audience: Scientists and clinicians interested in hyperpolarized gas magnetic resonance imaging (MRI).

Purpose: Previous work using hyperpolarized helium-3 (³He) MRI provides a strong foundation for the use of MRI in asthma research and patient care, however, a major drawback has been that we do not clearly understand the etiology of MRI-derived ventilation defects. We hypothesize that in asthma, ³He MRI ventilation abnormalities are related to airways that are remodeled and/or constricted. Therefore, in this proof of concept study, in a small group of asthmatic and healthy subjects, we quantitatively evaluated the relationship between hyperpolarized ³He MRI ventilation abnormalities and multi-detector x-ray computed tomography (MDCT) airway measurements in a region-of-interest (ROI) spatially identified by ³He MRI to contain ventilation defects.

Methods:

Subjects: Asthmatic and healthy subjects provided written informed consent to the study protocol approved by the local research ethics board and Health Canada and performed spirometry, plethysmography, MRI and MDCT. Subjects were enrolled between the ages of 18-60 years, with baseline forced expiratory volume in one second (FEV₁) > 60%_{pred}.

Image Acquisition: MRI was performed on a whole body 3.0 Tesla Discovery 750 scanner (General Electric Health Care, Milwaukee, WI, USA) in the coronal plane, as previously described (1). For ³He MRI static ventilation images, a fast gradient-recalled echo sequence was used (14 s breath hold; repetition time (TR) = 4.3 ms; echo time (TE) = 1.4 ms; flip angle = 7 degrees; field of view = 40 x 40 cm; matrix, 128 x 128; 14-17 slices; slice thickness = 15 mm; 0 mm gap). ³He gas was provided by a turn-key, spin-exchange polarizer system (HeliSpin, General Electric Health Care, Durham, NC, USA), with images acquired in breath-hold after inspiration of a 1 L ³He/N₂ mixture from functional residual capacity (FRC). ¹H MRI was acquired at a similar lung volume using a fast spoiled gradient echo sequence (16 s breath-hold; TR = 4.7 ms; TE = 1.2 ms; flip angle = 30 degrees; field of view = 40 x 40 cm; matrix, 128 x 128; 14-17 slices; 15 mm slice thickness; 0 mm gap). Following ³He MRI, thoracic CT was performed using a 64-slice Lightspeed VCT scanner (GEHC, Milwaukee, WI USA) using a detector configuration of 64x0.625 mm, 120 kVp, 100 effective mA, tube rotation time of 500 ms and a pitch of 1.0. In order to reduce the radiation dose delivered to each subject, CT images were acquired for 56 (versus a total of 400 possible) 1.25 mm thick slices in a non-random region-of-interest (ROI) spatially identified by ³He MRI to contain ventilation defects. In order to spatially register CT and ³He MRI breath-hold volumes and anatomy, CT was acquired similar to MRI with subjects in breath-hold after inhalation of 1.0L of N₂ from FRC.

Image Analysis: ³He MRI semi-automated segmentation was performed using custom software generated using MATLAB R2007b, as previously described (2). Briefly, ³He MRI was segmented using a K-means approach that classified voxel intensity values into five clusters ranging from signal void (cluster 1, C1 or ventilation defect volume (VDV)) to hyper-intense signal (C5), generating a ³He voxel cluster-map. For delineation of the ventilation defects from the thoracic cavity, the ¹H MRI thoracic cavity was segmented and ³He ventilation defect percent (VDP) was generated using VDV normalized to the thoracic cavity volume (TCV). This software enabled the segmentation of whole lung (WL) VDP as well as VDP in the ROI corresponding to the regional CT volume. The regional CT volume and ³He MRI were co-registered to quantify VDP and CT-derived airway measurements in the same anatomical region. Thoracic CT images were evaluated using commercial automated segmentation software (VIDA Diagnostics). Wall area percentage (WA%) and lumen area (LA) were quantified for the segmental bronchi within the regional CT volume. For each subject all airway segment measurements were averaged for the right and left lung separately to report whole lung averages. Either the right or left lung was evaluated based on the ability of the software to delineate and segment airways in the CT ROI. In the case where both lungs were evaluable, the lung side selection was randomized so that in total there were 9 left and 9 right asthmatic lungs (all from different subjects) as well as 3 left and 2 right healthy lungs.

Statistical Analysis: A multivariate analysis of variance (MANOVA) was performed using SPSS 20.0 (IBM, Armonk, NY, USA). Linear regression (r²) and Pearson correlation coefficients (r) were used to determine the relationship between CT and ³He MRI measurements using GraphPad Prism version 4.00 (GraphPad Software Inc, San Diego, CA, USA). Results were considered statistically significant when the probability of making a Type I error was less than 5% (p < 0.05).

Results: Subject characteristics and imaging measurements are provided in Table 1 for 18 asthmatics and 5 healthy subjects. Figure 1 shows the hyperpolarized ³He MRI static ventilation image and the regional CT of the centre coronal slice including regional measurements for WA%, LA and VDP for a healthy volunteer and two asthmatic subjects. As shown in Table 1, CT-derived measurements of regional WA% (p=.009) and LA (p=.01) were significantly different between asthmatics and healthy volunteers. Whole lung VDP (p=.01) and regional VDP (p=.02) were also significantly different between asthmatics and healthy volunteers. As shown in Figure 2, regional VDP was significantly correlated with WA% (r=.48, r²=.23, p=.02) and LA (r=-.51, r²=.26, p=.01).

Discussion: Taken together, these results suggest that there is a spatial structure-function relationship between airway morphological changes and ventilation defects, providing a better understanding of the underlying airway morphology related to heterogeneous ventilation abnormalities in asthma.

Conclusions: In a small group of asthmatic and healthy subjects, regional pulmonary CT measurements of airway wall thickness and lumen area were related to regional ³He MRI ventilation defects.

Table 1. Subject demographic characteristics, pulmonary function, ³He MRI and CT-derived airway measurements for asthmatic and healthy volunteers.

	Asthma n=18	Healthy n=5	Significance of Difference (p)
Age yrs	33 (11)	39 (12)	0.30
Male Sex	9	2	-
BMI kg/m ²	24 (4)	21 (2)	0.25
WL VDP	1.98 (1.06)	1.18 (0.35)	0.01
Regional VDP	1.50 (0.72)	0.93 (0.31)	0.02
WA%	67.6 (3.58)	62.7 (2.08)	0.009
LA mm ²	11.8 (5.28)	18.5 (1.83)	0.01

SD=Standard Deviation, BMI=Body Mass Index, VDP=Ventilation Defect Percent, WA%=Wall Area Percent, LA=Lumen Area. Significance of difference (p<.05) determined using a multivariate analysis of variance.

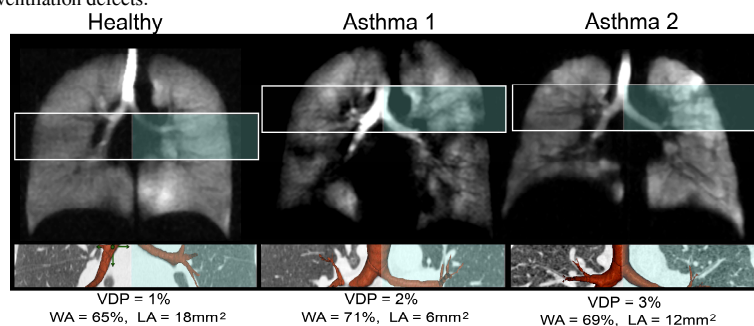


Figure 1. Regional hyperpolarized ³He MRI and CT for a healthy and asthmatic subject. The white box on the central coronal ³He static ventilation image shows the spatially registering CT-delineated ROI with the central coronal regional CT shown below. The lung side selected for analysis is highlighted in blue with the corresponding ³He and CT airway measurements shown below.

References: 1) Mathew, L. et al. *Eur J Radiol.* (2011), 2) Kirby, M. et al. *Acad Radiol.* (2012)

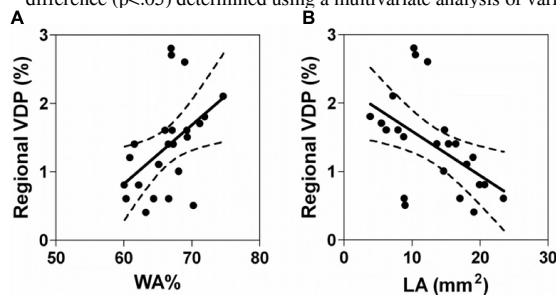


Figure 2. Relationship between regional ³He MRI ventilation defect measurements and CT airway measurements for all subjects. Regional VDP was significantly correlated with WA% (r=.48, r²=.23, p=.02) (A) and LA (r=-.51, r²=.26, p=.01) (B). Dotted lines represent the 95% confidence intervals of the regression line.